Determining the MTF of Medical Imaging Displays Using Edge Techniques

Amarpreet S. Chawla,[1] Hans Roehrig,[2] Jeffrey J. Rodriguez,[1] and Jiahua Fan[1]

The modulation transfer function (MTF) of a medical imaging display is typically determined by measuring its response to square waves (bar patterns), white noise, and/or line stimuli. However, square waves and white noise methods involve capture and analysis of multiple images and are thus quite tedious. Measurement of the line-spread function (LSF) offers a good alternative. However, as previously reported, low-frequency response obtained from the LSF method is not as good as that obtained from measurement of edge-spread function (ESF). In this paper, we present two methods for evaluating the MTF of a medical imaging display from its ESF. High degree of accuracy in the higher frequency region (near the Nyquist frequency of the system) was achieved by reducing the noise. In the first method, which is a variant of the Gans' original method, the periodic raster noise is reduced by subtracting a shifted ESF from the ESF. The second method employs a low-pass differentiator (LPD). A novel near maximally flat LPD with the desired cut-off frequency was designed for this purpose. Noise reduction in both the methods was also achieved by averaging over large portions of the image data to form the ESF. Experimental results show that the MTF obtained by these methods is comparable to that obtained from the square wave response. Furthermore, the MTFs of rising and falling edges of a cathode ray tube (CRT) were measured. The results show that the rising and falling vertical MTFs are practically the same, whereas the rising horizontal MTF is poorer than the falling horizontal MTF in the midfrequency region.

KEY WORDS: Cathode ray tube (CRT), liquid crystal display (LCD), modulation transfer function (MTF), edge-spread function (ESF), line-spread function (LSF), Gans' method, low-pass differentiator, image quality

INTRODUCTION

The relevance of image quality control of liquid crystal displays (LCDs) and cathode ray tubes (CRTs) for the purpose of soft-copy diagnosis has been well recognized, and several methods have been proposed for performing quality evaluation.[1–4] One common measure of performance is the spatial resolution of the imaging system, which is usually described by its modulation transfer function (MTF).

The conventional practice is to measure the MTF of an electronic display based on the response to square waves (bar patterns), lines, and white noise stimuli.[4] In these methods, an image of the portion of the display containing the test stimulus is captured using a charge-coupled device (CCD) camera. The MTF is then determined quantitatively by evaluating an ensemble of such images. However, the use of square waves is very labor-intensive. The MTF has to be assembled frequency by frequency from the output modulations of the fundamental and various harmonic frequencies in the spectra of usually 10 different spatial square waves used (one-on–one-off, two-on–two-off, ..., ten-on–ten-off), each of

which requires a separate image acquisition and analysis. Similarly, the method of measuring the response to white noise also entails acquisition of a large number of images and calculation of the noise power spectrum from each image to obtain a smooth MTF. Measurement of the MTF from the line-spread function (LSF) offers a good alternative, although it is prone to errors in calculation of a correction for the finite line width.[5] Moreover, it was shown by Cunningham and Reid[6] that measurement of the edge-spread function (ESF) yields superior response at low spatial frequencies than the LSF method.

The edge-based technique has been used for measuring the presampled MTF of digital radiographic systems, but to our knowledge, it has never been used to measure the MTF of a medical imaging display. In this article, we describe two methods to obtain the MTF of a CRT from its ESF.

The ESF is spatially unlimited because its end level differs from its starting level. Therefore it is typically differentiated to obtain the spatially limited LSF. The MTF is then deduced by Fourier transform methods. However, differentiators inherently boost the noise levels at higher frequencies.[7]

Several methods have been suggested to reduce the noise associated with the ESF method by low-pass filtering the ESF,[8] fitting the ESF to a parametric equation[9] or by local smoothing of the ESF.[10] In the latter approach, the ESF is oversampled and then smoothed by utilizing a fourth-order, Gaussian-weighted, moving polynomial fit. The order of the polynomial and the window size were deduced empirically, but a general solution was not derived in that work.

The two methods described in this article are designed to reduce the noise inherent in the calculation of the MTF from ESF. In the first method, which is a variant of the Gans' original method,[11] a shifted ESF is subtracted from the original (nonshifted ESF). Because of this subtraction, the high-frequency raster noise (not required for MTF measurement) of the display is considerably reduced. Fourier transform techniques are then applied to obtain the MTF. In the second method, a novel low-pass differentiator (LPD) was designed and used to obtain the LSF from the ESF. The LPD, which differentiates only low frequencies, ensures that the high-frequency noise does not contribute to the MTF. Furthermore, in both methods, signal averaging over a large portion of the edge is used to obtain an ESF with a satisfactory signal-to-noise ratio.

An additional aim of this project was to investigate the difference between the MTFs of rising and falling edges (called rising and falling MTFs for convenience) on a CRT. It was shown by Roehrig et al.[12] that compensation of the degradation caused by the display's MTF significantly improves its diagnostic image quality. However, their method ignores the differences between the behavior of rising and falling edges, and both types of edges have been incorrectly characterized with the same MTF. Knowledge of the difference in their MTFs can be used to further improve the image quality on a display by separately enhancing the rising and falling edges of the displayed image.

MATERIALS AND METHODS

The measurements were made on a high-performance monochrome CRT display with P45 phosphor and a pixel matrix of $2,560 \times 2,048$. The size of the CRT pixel (size of the Gaussian spot) was 0.144 mm; the Nyquist frequency was therefore 3.47 lp/mm. The CRT was set for a maximum luminance of 350 cd/m^2 and a minimum of 0.75 cd/m^2. Data were acquired with a CCD camera that recorded test images displayed by the CRT. The experimental setup is shown in Figure 1. The resolution of the CCD camera was $1,316 \times 1,036$ pixels at 6.8 μm. The magnification was such that that an array of 4×4 CCD pixels covered (sampled) one display pixel. This provided sufficient oversampling so that the effects of aliasing were minimal. Henceforth, for convenience, the term *magnification* will refer to the dimension of this 4×4 matrix of CCD pixels, 4 in this case. Figure 2 shows the actual output of a CCD camera imaging a rising horizontal edge on a CRT. Several 1-D profiles across the captured image were averaged to generate a single profile, which was then used for the MTF measurement. The resultant ESF then refers to this averaged 1-D profile of the edge.

ESF is not spatially limited. Direct application of discrete Fourier transform (DFT) on ESF therefore causes truncation errors. This is because the periodicity assumed by DFT causes abrupt transitions in the data.[7] DFT therefore cannot be directly applied to spatially unlimited ESF without introducing undesirable artifacts. This can be explained by considering a continuous-space rising horizontal step edge stimulus of infinite length. In theory, this will produce an ESF, $f_0(x)$, of infinite length and amplitude K, where x is the spatial coordinate and f_0 is the measured luminance, such that,

$$
\begin{aligned}
f_0(x) &= f_i(x), & x &< 0 \\
&= f_2(x), & 0 &\leq x < x_2 \\
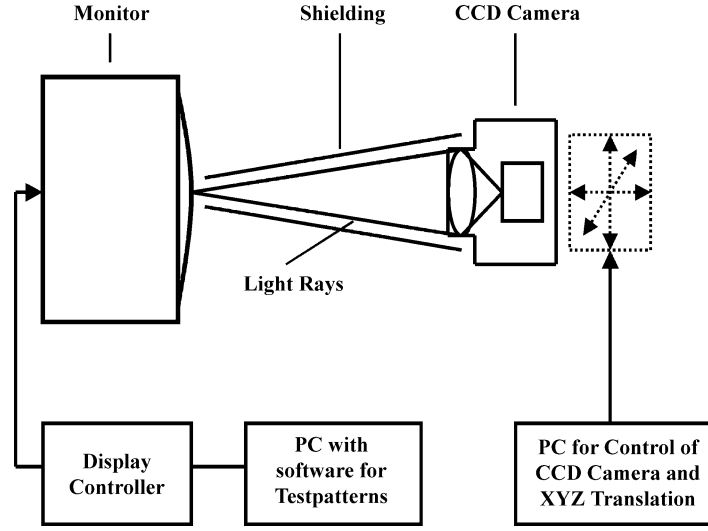&= f_f(x), & x &\geq x_2
\end{aligned}
\tag{1}
$$

Fig 1. Measurement of display performance parameters with a CCD camera.

where x denotes the position on the monitor, $f_i(x)$ is the function representing the initial part of the edge, $f_f(x)$ denotes the final part of the edge (of mean value K), and $f_2(x)$ (as shown in Figure 3) is the ESF captured by the CCD camera from the display within its observable field of view, $0 \leq x \leq x_2$. Clearly, $f_2(x)$ simply represents the truncated portion of the infinite edge $f_0(x)$, whose Fourier transform we are interested in. In a CRT, there will also be raster noise, which is periodic and synchronized with the display pixels, with approximately zero mean and small amplitude relative to the edge stimulus. Thus, the initial part of the ESF, $f_0(x)$, consists of just the raster noise and the final part consists of raster noise plus a constant offset (i.e., the plateau of the step edge).

Mathematically, the Fourier transform $F_2(j\omega)$ of the truncated edge $f_2(x)$ is given by

$$F_2(j\omega) = \int_{-\infty}^{+\infty} f_2(x)e^{-j\omega x}$$

$$= \int_{-\infty}^{+\infty} \left[f_0(x) - f_i(x) - f_f(x) \right] e^{-j\omega x} dx$$

$$= F_0(j\omega) - F_e(j\omega) \qquad (2)$$

where $F_0(j\omega)$ is the desired transform and $F_e(j\omega)$ is the erroneous term introduced by truncation of the edge function. Hence, $F_0(j\omega)$ can only be determined from this method if the error term $F_e(j\omega)$ is removed from $F_2(j\omega)$. This can be achieved by converting $f_0(x)$ into a spatially limited form.

In this section, the theoretical background behind the two methods used for measurement of the MTF will be discussed: a variant of the Gans' method and the low-pass differentiator method.

Gans' Method

$f_0(x)$ can be converted to a spatially limited form by subtracting a shifted version of the ESF from the original ESF, i.e.,

$$f_3(x) = f_0(x) - f_0(x - x_1), \;\; x_1 < x_2 \qquad (3)$$
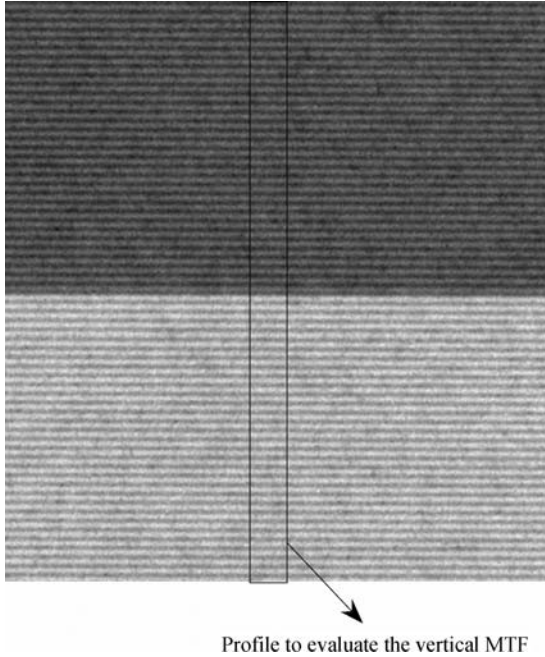

Profile to evaluate the vertical MTF

Fig 2. Actual output of a CCD camera imaging a rising horizontal edge on a CRT. Several profiles like the one drawn across the image are averaged to evaluate the MTF. (Contrast of the image has been enhanced so that the raster and noise can be clearly seen in the image.)
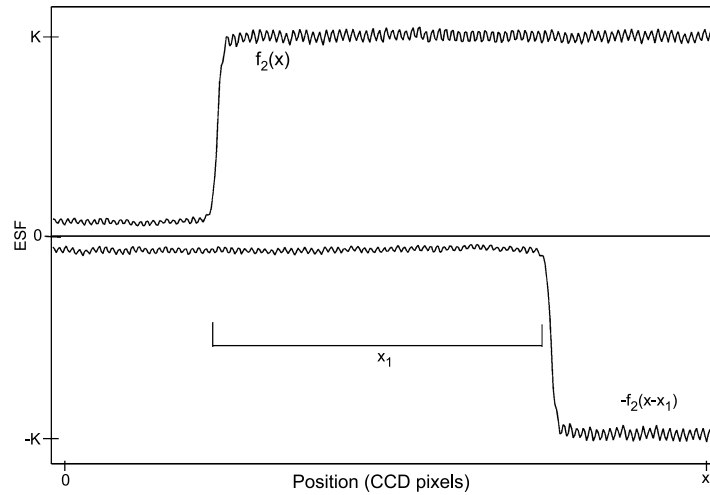
Fig 3. Portion of an infinite edge $f_0(x)$, denoted by $f_2(x)$, captured by a CCD camera along with its shifted version $-f_0(x - x_1)$, denoted by $-f_2(x - x_1)$. The sum of these two is $f_3(x)$.

The resultant function $f_3(x)$ is approximately zero outside the observable field ($x < 0$ and $x > x_2$) and therefore can be considered spatially limited within a reasonable approximation. Consequently, $f_3(x)$ (shown in Figure 4) can be represented as one period of a periodic waveform, thus allowing it to be represented by a Fourier series. The Fourier transform of $f_3(x)$ is given by

$$F_3(j\omega) = \int_{-\infty}^{+\infty} f_3(x)e^{-j\omega x}dx$$

$$= \int_0^{x_2} f_3(x)e^{-j\omega x}dx$$

$$= F_0(j\omega)\left[1 - e^{-j\omega x_1}\right]$$

$$= F_0(j\omega)[1 - (\cos \omega x_1 - j \sin \omega x_1)]$$

$$\Rightarrow |F_3(j\omega)| = 2|F_0(j\omega)| \sin(\omega x_1/2) \tag{4}$$

$|F_0(j\omega)|$ can then be found from $|F_3(j\omega_n)|$ at all frequencies ω. In particular, if $x_2 = 2x_1$, at frequencies $\omega_n = n\pi/x_1$,

$$|F_3(j\omega_n)| = 2|F_0(j\omega_n)|, \qquad n = \pm 1, \pm 3, \pm 5, \ldots$$
$$= 0, \qquad n = \pm 2, \pm 4, \pm 6, \ldots \tag{5}$$

Therefore, as shown in Figure 5, the MTF can be calculated by dividing $F_3(j\omega)$ by the input modulation at each discrete frequency ω_n.

Because the value of discrete frequency ω_n depends on the shift x_1, the edge can be shifted by different values to obtain all the frequency points of interest. To obtain the MTF, we simply divide $f_3(x)$ by the corresponding input—i.e., a difference of two ideal step functions, or a rectangular pulse. Hence, for any other shift $x_2 \neq 2x_1$, the MTF can be directly derived from $f_3(x)$ by dividing $|F_3(j\omega)|$ by a sinc function (Fourier transform of an ideal rectangular pulse[13]), except at frequencies where the sinc function is singular, i.e.,

$$MTF(\omega) = \frac{|F_3(j\omega)|}{x_1 \text{ sinc}(x_1\omega/2\pi)}, \ \omega \neq 2n\pi/x_1; \ n = \pm 1, \pm 2, \ldots \tag{6}$$

Differentiator

Because differentiation of a signal gives an estimate of its rate of change, the ESF can alternatively be differentiated to obtain the LSF.[6] To obtain the MTF, the LSF is Fourier-transformed, corrected for the finite line width, and normalized at DC to a value of 1.

The ideal differentiator has a magnitude response that is proportional to the frequency. It has the following frequency response:

$$H(\omega) = j\omega, |\omega| \leq \pi \tag{7}$$

Sources of significant high-frequency noise on CRTs and LCDs are, respectively, raster effects and fluctuations in the luminance level resulting from interspaced dark regions between pixels. As a result of oversampling by the CCD camera (4 pixels capture 1 CRT pixel), frequencies four times the Nyquist frequency of the display are acquired. The high-frequency components extending beyond the Nyquist frequency of the monitor do not contribute to its MTF and hence need to be removed. However, an ideal differentiator (shown as "ideal response" in Figure 6) amplifies undesirable high-frequency noise because of its high-pass characteristics.[7]
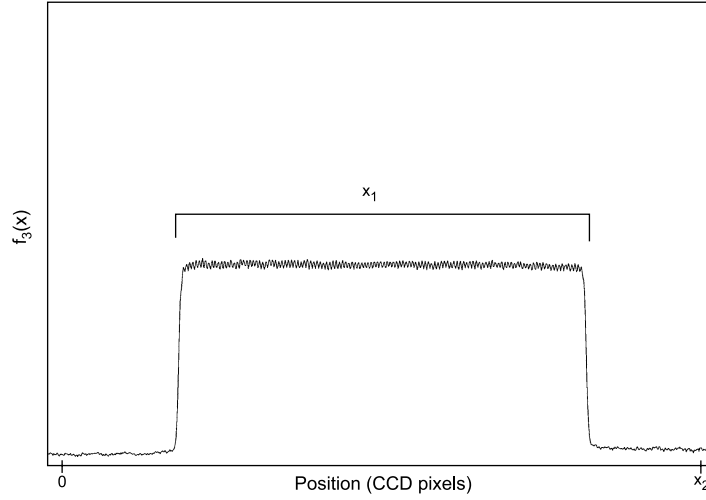
Fig 4. $f_3(x)$**. As desired,** $f_3(x)$ **is spatially limited. At certain discrete frequencies, the magnitude of its Fourier transform is related to that of a spatially unlimited edge with a constant.**

In practical implementations, the ideal differentiator must be approximated because the ideal impulse response has infinite length. The differentiators commonly used are approximated by difference operations where the input–output relation is simply given by $y(n) = x(n) - x(n - 1)$ (Samulson's differentiator) or $y(n) = a[x(n + 1) - x(n - 1)]$ (central-difference algorithm), where a is a constant factor.[10] The corresponding frequency responses are given by

$$H(\omega) = 1 - \cos(\omega) + j\sin(\omega) \quad \text{and}$$
$$H(\omega) = a[2j\sin(\omega)] \tag{8}$$

Although Samulson's differentiator and the transfer function of Gans' method described in the previous section are identical for the case when $x_1 = 1$ in (Equation 4), Samulson's

differentiator is an all-pass differentiator. Unlike Gans' method, where the noise is reduced due to subtraction of two images with shifted edges, Samulson's differentiator boosts high frequencies and, hence, also the noise. The central-difference algorithm with frequency response given in Equation (8) closely approximates Equation (7) for very low frequencies (approximately until $\pi/7$, for certain values of a), as shown in Figure 6, and then deviates from the ideal behavior. Even for the best-case scenario of $a = 0.5$, the frequencies from approximately $\pi/7$ until $\pi/2$ are not linearly boosted. This not only causes unexpected error in the output, but also boosts unwanted high-frequency noise. Therefore, if Samulson's simple differentiator or the central-difference algorithm is applied to an ESF obtained from an LCD or CRT display, high-frequency noise will be amplified, producing errors in the obtained MTF.
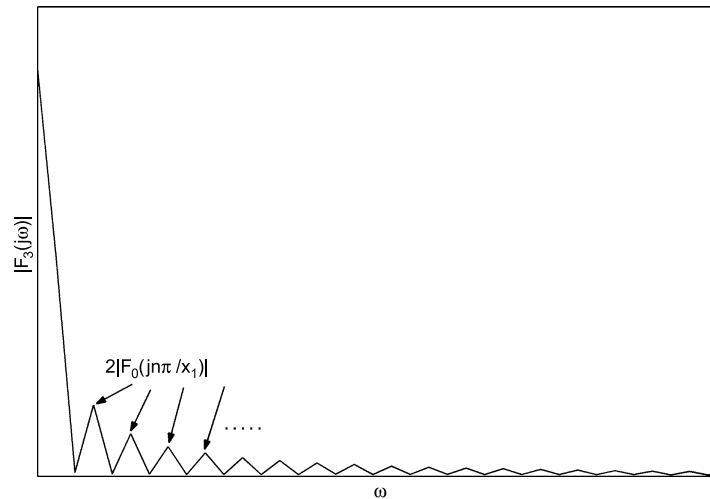

Fig 5. Magnitude of the Fourier transform of $f_3(x)$**, which is exactly equal to twice that of an infinite edge at certain discrete frequencies if** $x_2 = 2x_1$**.**
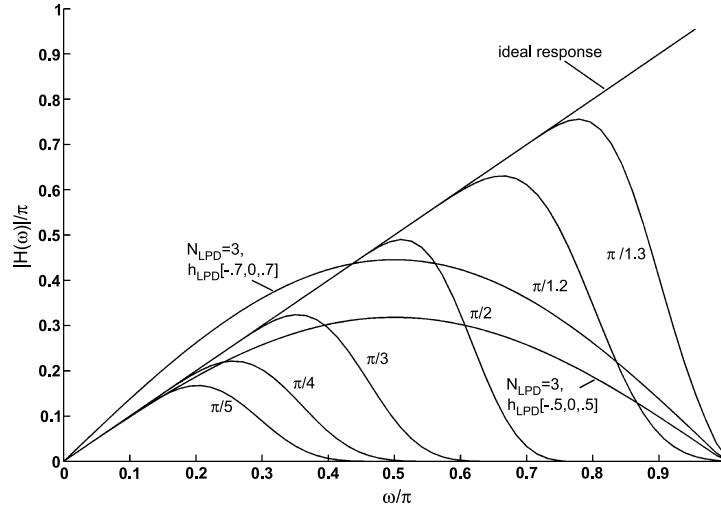
Fig 6. Magnitude response of an LPD designed via the window method for N = 31 and different cut-off frequencies.

One way to reduce the noise is to apply a low-pass filter to the ESF and then differentiate it in two cascaded stages of filter. Alternatively, these can be combined into a single linear filter—a low-pass differentiator (LPD). An ideal LPD has a desired frequency response given by

$$H_{LPD}^d(\omega) = \begin{cases} j\omega, & |\omega| \leq \omega_c \\ 0, & \omega_c < |\omega| \leq \pi \end{cases} \quad (9)$$

where ω_c (cut-off frequency) denotes the upper limit of the differentiator band. Such a filter behaves as a differentiator in the frequency range $[0, \omega_c]$ and attenuates the higher frequency components.

A digital filter of length N can be represented by the transfer function,

$$H(z) = \sum_{n=0}^{N-1} h(n)z^{-n} \quad (10)$$

where $h(n)$ is the impulse response of the filter. In the design of the LPD, the impulse response of the filter, h_{LPD}, is required to be antisymmetric because the frequency response of such a filter, as indicated in Equation (9), is imaginary. A causal Type III filter,[13] whose length (N) is odd, is designed in this paper. Thus, we have

$$h_{LPD}(n) = -h_{LPD}(N-1-n), n = 0, 1, \dots (N-3)/2 \quad (11)$$

and

$$h_{LPD}\left(\frac{N-1}{2}\right) = 0 \quad (12)$$

Consequently, the frequency response of the filter is given by

$$\tilde{H}(\omega) = e^{-j(N-1)\omega/2} e^{j\pi/2} M(\omega), |\omega| \leq \pi \quad (13)$$

where

$$M(\omega) = \sum_{k=1}^{(N-1)/2} c(k) \sin(k\omega) \quad (14)$$

and

$$c(k) = 2h_{LPD}[(N-1)/2 - k] \quad (15)$$

In the past, LPDs have been designed using the Remez algorithm (essentially minimizing the relative error),[14] using relative mean-square error minimization,[15–17] and using the Kaiser window.[18] Recent works have been published proposing a maximally flat LPD.[19] In our work, the LPD is designed using the window method. However, unlike the method of Wong and Antoniou,[18] which utilizes an empirically chosen shape parameter β for the Kaiser window and which causes a slight shift in the resultant cut-off frequency, the value of β is determined iteratively, which results in a filter that closely approximates a maximally flat differentiator with a cut-off frequency being exactly ω_c. The design of such a differentiator is discussed in the following subsection.

LPD Designed by the Window Method

Because the desired frequency response of an LPD, $h_{LPD}^d(\omega)$, is known, it is possible to determine the desired impulse response of the filter, $h_{LPD}^d(n)$, by obtaining the inverse Fourier transform of $h_{LPD}^d(\omega)$. Thus,

$$\begin{aligned} h_{LPD}^d(n) &= \frac{1}{2\pi} \int_{-\omega_c}^{\omega_c} j\omega e^{j\omega_n} d\omega \\ &= \frac{-j}{2\pi n^2} \left[e^{j\omega_c n}(j\omega_c n - 1) - e^{-j\omega_c n}(-j\omega_c n - 1) \right] \\ &= \frac{\omega_c}{\pi n} \cos(\omega_c n) - \frac{1}{\pi n^2} \sin(\omega_c n), \, n = 0, 1, \dots (N-3)/2 \end{aligned}$$

$$(16)$$

Because such a filter is infinite in length, a finite impulse response (FIR) filter is obtained by multiplying $h_{LPD}^d(n)$ by a window function, $w(n)$:

$$h_{LPD}(n) = h_{LPD}^d(n)w(n) \qquad (17)$$

Here, h_{LPD} is required to be antisymmetric so its frequency response $\widetilde{H}(\omega)$ satisfies Equations (13–15). Common window functions were investigated, including, among others, the rectangular window, Hanning window, Hamming window, and the Kaiser window. The Kaiser window, which is a near-optimal window in terms of the trade-off between the mainlobe width and sidelobe area,[13] was used for the present application. However, the shape parameter β *cannot* be found by minimizing the mean squared error because this criterion leads to adverse behavior at ω_c, where $h_{LPD}^d(\omega_c)$ is discontinuous.[13] The value of β was instead determined iteratively, such that first, $\widetilde{H}(\omega)$ is linear at $\omega = 0$, and second, its magnitude response is maximum at $\omega = \omega_c$. The first condition requires that

$$\frac{d}{d\omega}M(\omega) = 1, \omega = 0 \qquad (18)$$

Hence, the coefficients c in Equation (14) (forcing the condition of Equation 18 on Equation 15) are given by

$$c(1) + 2c(2) + \cdots + \frac{(N-1)}{2}c\left(\frac{N-1}{2}\right) = 1 \qquad (19)$$

The second condition requires that

$$\frac{d}{d\omega}M(\omega) = 0, \ \omega = \omega_c \qquad (20)$$

In order for the above statement to be true, the coefficient c must satisfy

$$c(1)\cos(\omega_c) + 2c(2)\cos(2\omega_c) + \cdots$$
$$+ \frac{(N-1)}{2}c\left(\frac{N-1}{2}\right)\cos\left(\frac{N-1}{2}\omega_c\right) = 0 \qquad (21)$$

Values of β that satisfy the first criterion in Equation (18) shift the effective cut-off frequency away from ω_c in the resultant filter. Therefore, the cut-off frequency in Equation (16) was tuned iteratively to satisfy the second criterion (Equation 21). Because of the rather severe constraints on the slope of $\widetilde{H}(\omega)$, it was found that its magnitude deviates from the desired response at the cut-off frequency (magnitude is less than ω_c at ω_c). Therefore, a lower limit was set for the magnitude of $\widetilde{H}(\omega)$ at the cut-off frequency. We found that a limit of -3 dB usually guarantees a solution. As shown in Figure 6, the resultant filter is maximally flat at $\omega = \pi$ for low cut-off frequencies, i.e.,

$$\frac{d^m}{d\omega^m}M(\omega) = 0, \ \omega = \pi; \ \ m = 2, 3, \ldots 2N - 3 \qquad (22)$$

FILTER DESIGN EXAMPLES

An LPD with a specific length (N) and cut-off frequency (ω_c) was designed by the method described in the previous section. Figure 6 shows the frequency response of a family of differentiators with constant N and different cut-off frequencies. Because only Type-III differentiators were designed, N is a positive odd integer. For comparison with maximally flat LPDs designed by Selesnick,[19] N was chosen to be equal to 31. The differentiators satisfy Equations (18) and (20), and hence are linear at $\omega = 0$ and their magnitude response peaks at the desired cut-off frequency. Although the resultant filter is not maximally linear at $\omega = 0$ (not satisfying Equation 8 in Ref. 19), the third derivative was reasonably close to 0. For low cut-off frequencies, the differentiators are maximally flat at $\omega = \pi$, satisfying Equation (22). The value at the cut-off frequency was within the ± 3 dB limit of the desired response. This value improves by choosing larger values of N, as illustrated in Figure 7, where differentiators of different orders and the same desired cut-off frequency, $\pi/4$, are plotted. As illustrated, higher values of N cause a sharper transition into the stop band. Figure 6 also shows the frequency response of a third-order differentiator with impulse response,

$$h_{LPD} = a[1, 0, -1], \ a \in (0, 1) \qquad (23)$$

As can be seen, the response of such a filter is linear at low frequencies only if $a = 0.5$. At other values of a, the resultant differentiator rapidly deviates from the ideal response even at very low frequencies. Also, such differentiators have a fixed cut-off frequency of $\pi/2$ and, hence, will continue to boost frequencies until $\pi/2$ even if they lie beyond the Nyquist frequency of the system. Furthermore, because not all the frequencies up to $\pi/2$ are linearly boosted, there are errors in filter's output, as explained in the next section.

EXPERIMENTAL RESULTS

The MTF derived from the edge response was compared to that obtained from the square wave response. For quantitative purposes, the normalized mean squared error (NMSE) was computed be-
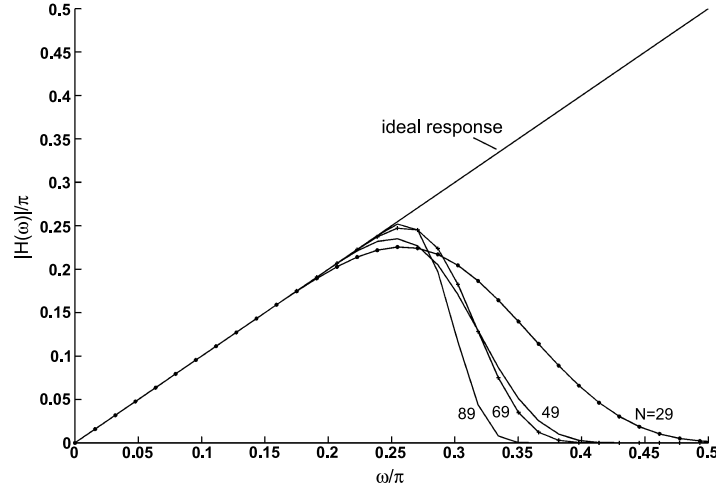
Fig 7. Magnitude response of an LPD designed by the window method for the same cut-off frequency $\pi/4$ and different N.

tween the two MTFs and is presented in Table 1. The NMSE is given by

$$NMSE = \frac{1}{N_{nyquist}} \sum_{k=1}^{N_{nyquist}} \left[\frac{MTF_{sq.wave}(f_k) - MTF_{edge}(f_k)}{MTF_{sq.wave}(f_k)} \right]^2$$

(24)

where $N_{nyquist}$ is the number of frequency points up to the Nyquist frequency of the display at which the MTF is sampled. As the MTF from the square wave response is sampled at very few points,[5] it was interpolated with a fifth-order polynomial. Most imaging systems have low-pass characteristics, so the NMSE provides greater weight to the error in the high-frequency region. Because the edge-based method of MTF estimation is expected to boost noise at high frequencies, the NMSE is well suited for evaluating the performance.

Because rising and falling edges have different MTFs (as discussed in Rising and Falling Edges), horizontal and vertical MTFs were computed by averaging the rising and falling edge response in the respective directions.

Gans' Method

The 1-D profile of the image with original (nonshifted) ESF [denoted by $f_2(x)$ in an earlier section and in Figure 3] was analyzed. The length of $f_2(x)$ was $2x_1$ (i.e., in Figure 3, $x_2 = 2x_1$). If the edge in the original ESF is at $x_1/2$, a shift of $f_2(x)$

by x_1 would result in a shifted ESF, $f_2(x - x_1)$, with the edge at $3x_1/2$. One can also shift the edge by $x_1/2$. Because the edge on the display can be shifted only by integral values, $x_1/2$ is required to be a multiple of the magnification value. For a magnification of 4 and a horizontal edge, the value of x_1 that satisfies this condition (and which provides the highest resolution in the frequency domain) was found to be 512. Similarly, for a vertical edge, x_1 was 656.

Three images, one with the original ESF with edge at $x_1/2$, and the other two with edges shifted to x_1 and $3x_1/2$, were acquired by the CCD camera. It must be noted that the 1-D profile of the image with the original ESF was subtracted from the 1-D profile of the image with the shifted edge instead of actually shifting the edge $f_2(x)$

Table 1. Normalized mean squared error between vertical MTF derived from ESF and square-wave response

N_{LPD}	ω_c			
	$\pi/5$	$\pi/6$	$\pi/7$	$\pi/8$
27	0.5643	0.2788	0.0228	0.0564
29	0.5704	0.1448	0.0142	0.0537
31	0.5697	0.2562	0.0197	0.0568
33	0.6072	0.2353	0.0289	0.0609
39	0.8550	0.1140	0.0533	0.0597
49	0.7912	0.2110	0.0708	0.1605

The ESF was differentiated by an LPD designed via the window method. ω_c indicates the cut-off frequency of such a filter, and N is its length. The corresponding error obtained from a filter with impulse response $h_{LPD} = [0.5, 0, -0.5]$ is 1.331.
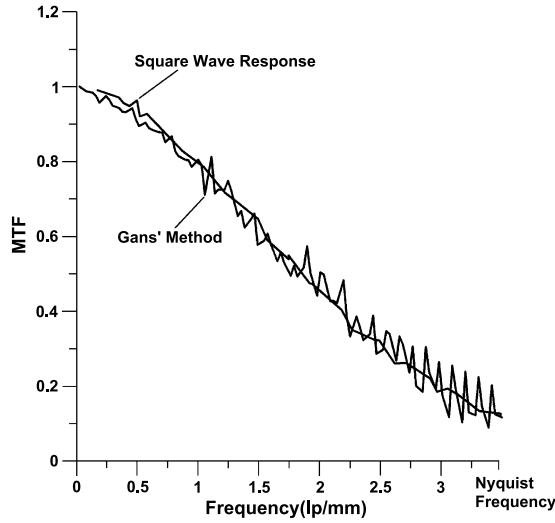
Fig 8. Comparison of vertical MTFs obtained from ESF and square wave response. Gans' method was applied to determine the MTF from the ESF. (Nyquist frequency = 3.47 lp/mm.) NMSE = 0.0241.

MTF is obtained by dividing the output modulation by the input modulation (an ideal edge is the input) and correct normalization. Figure 8 shows the MTF obtained by Gans' method. The MTF from the square-wave response has also been shown for comparison purposes. The NMSE is 0.0241.

LPD Designed by Window Method

The line-spread function (LSF) can be derived from the ESF by differentiating it. The ESF was obtained from a single image acquisition by the CCD camera. It was differentiated with an LPD to obtain an LSF. Figure 9 shows LSFs obtained using an LPD of length 29 and different cut-off frequencies. In the figure, the raster frequency representing high-frequency noise on a CRT is suppressed. An FFT is then applied to the LSF. Correction for finite line width on the CRT is then applied and the MTF derived. To perform the differentiation, LPDs of different lengths and cut-off frequencies were designed by the window method. The resultant MTFs were compared to that obtained from the square wave response. As shown in Figures 10 and 11, only a filter length of 29 and a cut-off frequency (ω_c) of $\pi/7$ result in an MTF equivalent to that obtained from the square wave response. As illustrated in Table 1, such a filter results in a minimum NMSE of 0.0142 in the obtained MTF. Increasing the value of N or ω_c increases the error.

by x_1 and subtracting from itself as originally suggested by Gans and Nahman.[11] The DFT was applied to the resultant subtracted profile, which is the shape of a rectangular function, as shown in Figure 4. Then as explained in Equation (5), at certain discrete frequencies the magnitude of the Fourier transform is twice that of the original edge. The two shifted edges yield two different sets of such discrete frequency points, which are assembled to obtain the output modulation. The
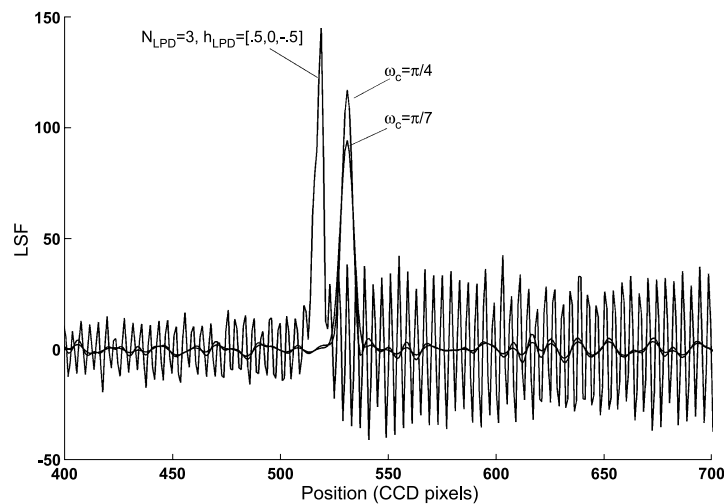

Fig 9. LSF obtained after differentiating an edge using an LPD with N = 29 and various cut-off frequencies.
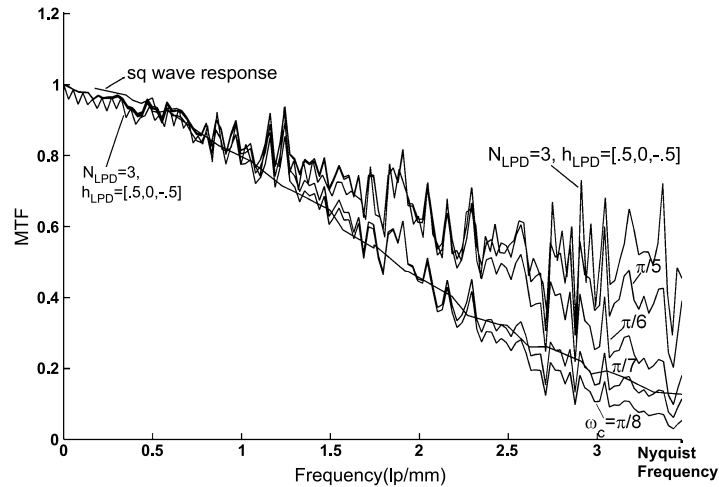
Fig 10. Comparison between vertical MTFs derived from ESF and square wave response on a 5-megapixel, high-precision CRT at luminance of 37 cd/m^2 (Nyquist frequency = 3.47 lp/mm). The ESF was differentiated by an LPD (N = 29) designed via the window method. The filter with $\omega_c = \pi/7$ gives the least deviation of the MTF from the square wave response.

Rising and Falling Edges

MTFs of rising and falling edges in both the vertical and horizontal directions were determined. As shown in Figure 12, MTFs of rising and falling edges on a CRT are different. Although the vertical MTFs (for horizontal edges) remain practically the same, the horizontal falling and rising edges show significant differences. It has been shown by Chawla et al.[5] that on LCDs, the rising and falling MTFs are practically the same.

As shown in Figure 13, the horizontal edge has the same falling and rising characteristics. However, the falling vertical edge in Figure 13(a) has a much steeper transition than the rising vertical edge. This has direct implications in the horizontal MTF. As seen in Figure 12, the horizontal rising MTF has a considerable drop in the midfrequency region as compared to the horizontal falling MTF.

As noted by Compton,[20] "the electron optics controls the vertical dimension and the video amplifier controls the horizontal dimension of each
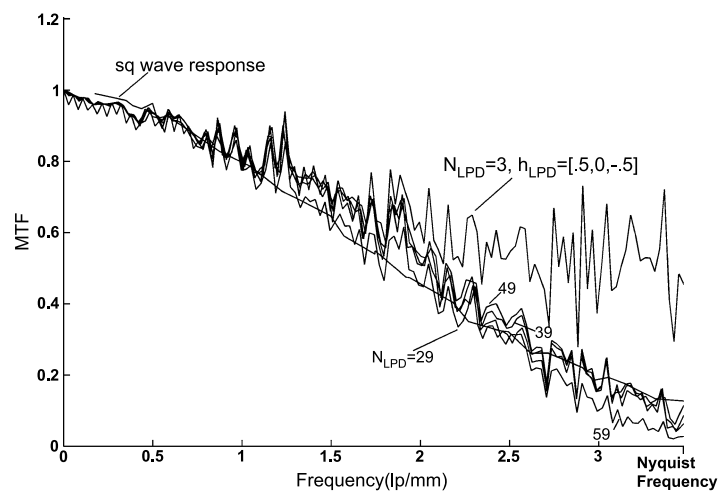

Fig 11. Comparison between vertical MTFs derived from ESF and square wave response on a 5-megapixel, high-precision CRT (Nyquist frequency = 3.47 lp/mm). The ESF was differentiated by an LPD ($\omega_c = \pi/7$) designed by the window method. The filter with N = 29 gives the least deviation of the MTF from the square-wave response.
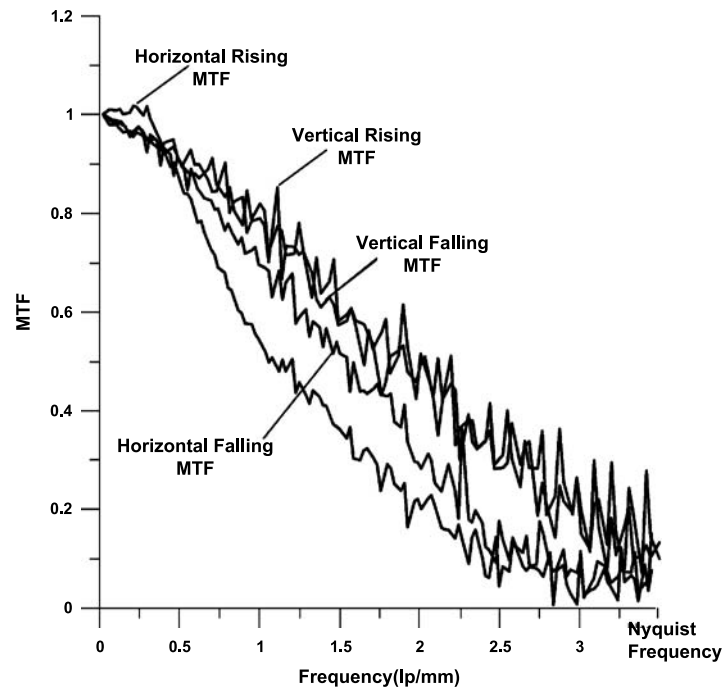
Fig 12. Comparison of horizontal/vertical MTFs obtained from rising and falling ESFs on a 5-megapixel, high-precision CRT at luminance of 37 cd/m^2 (Nyquist frequency = 3.47 lp/mm).

pixel. The ability of the video amplifier to transition from one command level to another is the determining factor controlling the pixels' width and profile." It can therefore be concluded that the significant differences in the rising and falling horizontal MTFs are caused by differences in the rising and falling times of the video amplifier. The phosphor used in a CRT is not part of the pixel spread associated with the amplifier's response. Phosphors are all but instantaneous turning on.

DISCUSSION

The edge response of a 5-megapixel, high-performance monochrome CRT was determined using a variant of Gans' method and the differentiator technique. Because square waves, lines, and white noise yield practically identical MTFs,[4] the MTFs obtained via the edge response were compared only to that obtained from the square wave response.

Gans' method requires the image of the shifted edge to be subtracted from the image of the original edge. This direct subtraction was found to be an effective way of reducing the raster noise,

which on a CRT is predominantly periodic and synchronized with the display pixels. The variance (i.e., noise power, or the area under the power spectral density curve) in the lower and upper levels of the original edge ($f_2(x)$) on a CRT was 184.6 and 352.3, respectively. On the other hand, it was 28.2 and 116.4, respectively, in the lower and upper levels of $f_3(x)$. It should be noted that the performance of Gans' method depends on how well the periodic structures in the two images are aligned so that they are cancelled when the two images are subtracted. Misalignment may introduce high-frequency noise in the subtracted image. Proper alignment is also necessary for $f_3(x)$ in Figure 4 to be approximated as spatially limited. Improper alignment may occur as a result of mechanical jitters in the CCD camera while capturing the images and/or the raster jitter on a CRT.

The differentiator technique has traditionally been used to obtain the MTF from the ESF. However, because differentiating boosts high frequencies, the ESF has typically been used to determine only the low-frequency response of the system. However, application of an LPD to differentiate the ESF not only preserves the low-frequency response of the system but also gives a
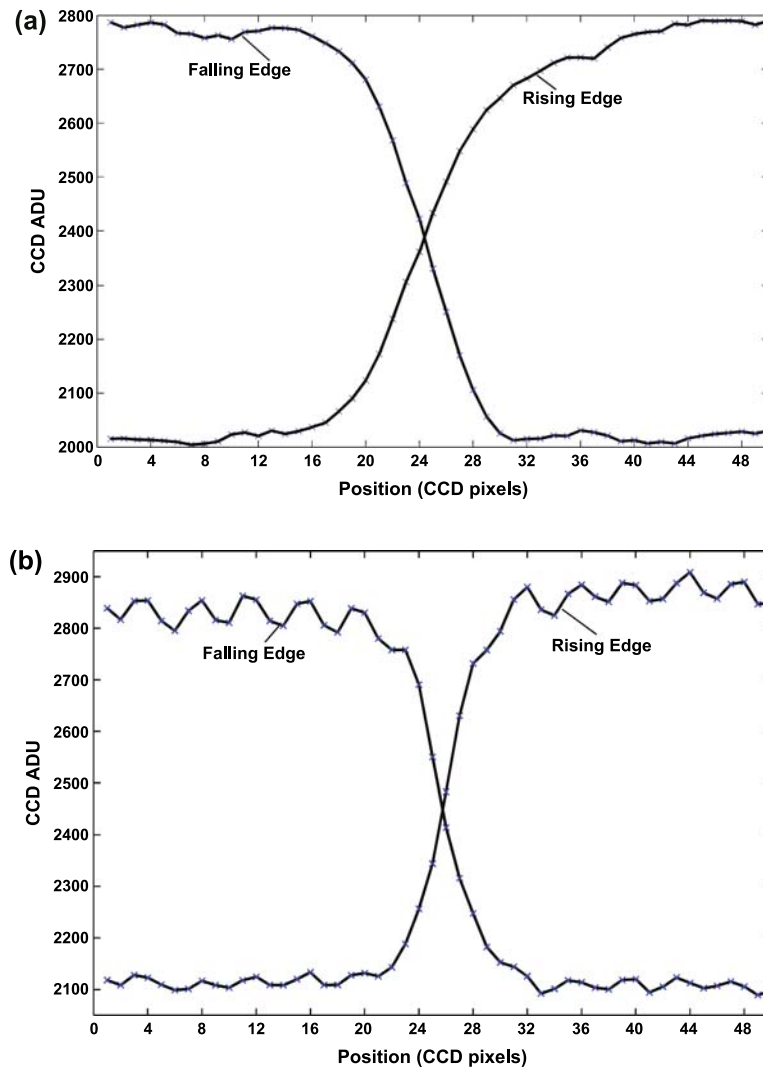
Fig 13. Comparison of falling and rising vertical/horizontal edges. Whereas a steeper transition in falling vertical edge makes horizontal falling MTF better than the horizontal rising MTF (in the mid-frequency region), such a difference is not seen in falling/rising horizontal edge. Consequently, vertical MTFs of falling/rising edges are practically the same (as illustrated in Figure 12).

reasonably correct estimate of the high-frequency response with a proper combination of N and ω_c. This is shown in Figures 10 and 11. A right combination of N and ω_c is important because different values of the two parameters can cause deviation from the actual response in the high-frequency region. A filter with a higher value of ω_c, as illustrated in Figure 6, differentiates over a greater frequency range and hence boosts higher frequencies. This is the reason why a filter with a cut-off frequency of $\pi/7$ gives the least error (Fig 10), although the Nyquist frequency of the oversampled system (oversampled by 4) is $\pi/4$. In

general, a higher value of ω_c causes larger deviations of the MTF from the square wave response at the Nyquist frequency.

As the performance of a filter, in general, improves by increasing its length, one might expect that higher values of N will reduce the error in the obtained MTFs. This, as illustrated in Figure 11, may not be true because higher values of N cause an increase in spread of the LSF obtained by differentiating the ESF. As seen in Figure 7, the filter with a higher value of N has a sharper transition into the stop-band further attenuating the higher frequencies, which in turn has the effect of an
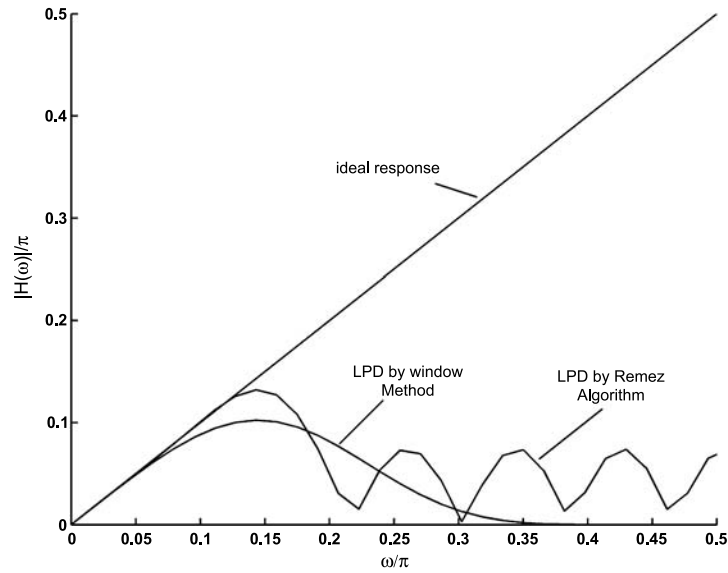
Fig 14. Comparison between LPDs designed via the window method and the Remez algorithm.

increase in the spread of the LSF in the spatial domain. This can also be understood by considering that the output of convolution of a signal of length K with a filter of length N has resulting length $K + N − 1$.

The highest NMSE (1.331), however, is given by a differentiator with impulse response $h =$ [0.5, 0, −0.5]. Even in the low-frequency range, the MTF obtained by this differentiator is very noisy and provides a slightly different low-frequency response than either of the LPDs or the square wave response. It may be safely concluded that this

differentiator will not provide a faithful measurement of the frequency response of a system as much as the LPDs, even at low frequencies.

The LPD designed with the window method was compared with one designed with the Remez algorithm. The filters designed with the Remez algorithm are optimal in the sense that the maximum error between the desired frequency response and the actual frequency response is minimized according to the "minimax" criterion.[14] However, the Remez algorithm does not give an optimal filter if other criteria such as the "maximally flat" or
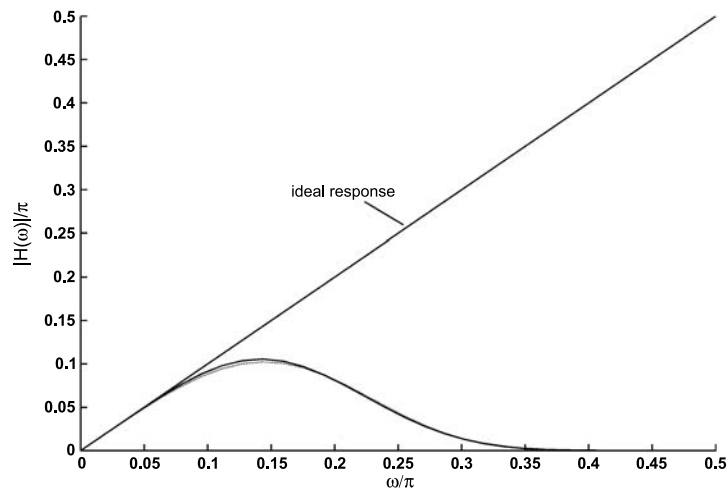

Fig 15. Comparison of near-maximally at LPDs designed via the window method and the Remez algorithm.

"least-squared error" are used. For a fixed filter length, Remez-designed LPD with greater linearity in the pass-band will have greater ripple in the stop-band. For example, as shown in Figure 14, for the same filter length $N = 29$, transition band of [0.4, 0.6] rad/s, $\delta_1 = 0.085$ and $\delta_2 = 0.280$ in the pass-band and the stop-band, respectively, and the same cut-off frequency $\pi/7$, the Remez filter is more linear than the window-designed filter in the pass-band. However, the stop-band error in the Remez-designed filter is equiripple as compared to the stop-band error in the window-designed filter, which decreases toward the Nyquist frequency. Consequently, the LPD designed by the Remez algorithm yields a higher NMSE of 0.0575 in the resultant MTF compared to 0.0142 for the LPD designed by the window method. If we allow the transition band to be very wide, it is possible to derive an LPD from the Remez algorithm with nearly the same frequency response as the LPD derived from the window method. This is shown in Figure 15. The transition band for this Remez filter is [0.04, 1.48] rad/s (for a cut-off frequency of $\pi/7$). Although δ_1 and δ_2 in this case are 8.5×10^{-16} and 2.8×10^{-10}, respectively, the NMSE in the MTF derived by such an LPD is still 0.0183, which is larger than the NMSE of 0.0142 obtained by the LPD designed by the window method.

Although the LPD method achieves the lowest NMSE (0.0142) in the MTF as compared to 0.0241 for Gans' method, the latter is easier to implement. This is because the order (N) and cut-off frequency (ω_c) of an LPD for an accurate measurement are presently determined empirically. However, as these two parameters depend strictly on the Nyquist frequency of the display, the LPD offers promising technique for noise reduction. Because of the convenience in data acquisition and analysis in both the methods, they can be used for obtaining the MTFs of electronic displays in real-time.

CONCLUSIONS

The MTF of a high-precision CRT used for display of high-resolution medical images was determined from its edge response. Two methods were employed for this purpose: (1) a variant of Gans' original method and (2) a low-pass differentiator (LPD) that combines the behavior of a differen-

tiator and a low-pass filter. The MTF can be accurately estimated over all frequencies up to the Nyquist frequency of the system. The two methods achieve this by reducing the high-frequency noise associated with the ESF method. The MTF obtained is comparable to that obtained from the square wave response, but is less labor-intensive than the square wave technique.

MTFs of rising and falling edges of a CRT were measured. It was found that the rising and falling horizontal MTFs were remarkably different. This may be a result of insufficient bandwidth of the video amplifier to support the high density of high-resolution (5 megapixels) diagnostic CRTs. The rising and falling vertical MTFs were practically identical.

Although the two methods described in the paper to determine the MTF from the ESF have been applied to images of a CRT, they can also be used to determine the MTF of LCDs. However, as the MTF of LCDs is almost perfect, the MTF of CRTs offers more interesting study.

ACKNOWLEDGMENTS

REFERENCES

1. Samei E, Badano A, Chakraborty D, Compton K, Cornelius C, Corrigan K, Flynn MJ, et al: Assessment of Display Performance for Medical Imaging Systems. Draft Report of the American Association of Physicists in Medicine (AAPM) Task Group 18. (URL: http://deckard.mc.duke.edu/~samei/tg18_files/tg18.pdf)

2. Roehrig H, Charles EW, Damento MA: Characterization of monochrome CRT display systems in the field. J Digit Imaging 12(4):152–165, Nov. 1999

3. Roehrig H, Dallas WJ, Blume H, Sivarudrappa M: Software for CRT image quality evaluation. Proc SPIE 3976:442–453, 2000

4. Roehrig H, Chakraborty DP, Fan J, Chawla A, Gandhi K: "The Modulation Transfer Function (MTF) of CRT Display Systems." In: Proceedings of the Department of Defense Breast Cancer Research Program Meeting, ERA OF HOPE, vol. 2, Poster Session 28, Sept. 25–28, 2002

5. Chawla AS, Roehrig H, Fan J, Gandhi K: "Real-time MTF evaluation of displays in the clinical arena. Proc SPIE 5029(84), 2003

6. Cunningham IA, Reid BK: Signal and noise in modulation transfer function determinations using the slit, wire, and edge techniques. Med Phys 19:1037–1044, 1992

7. Waldmeyer J: "Fast Fourier transform for step-like functions: the synthesis of three apparently different methods." IEEE Trans Instrum Meas IM-29(1), 1980

8. Jones RA, Yeadon EC: Determination of the spread function from noisy edge scans. Photogr Sci Eng 13:200–204, 1969

9. Boone JM, Seibert JA: An analytical edge spread function model for computer fitting and subsequent calculation of the LSF and MTF. Med Phys 21:1541–1545, 1994

10. Samei E, Flynn MJ, Reimann DA: A method for measuring the presampled MTF of digital radiographic systems using an edge test device. Med Phys 25:102–113, January 1998

11. Gans WL, Nahman NS: Continuous and discrete Fourier transforms of step-like waveforms. IEEE Trans Instrum Meas IM-31:97–101, 1982

12. Roehrig H, Dallas WJ, Krupinski E, Fan J, Chawla AS, Gandhi K: "Display of mammograms on a CRT." In: 6th International Workshop on Digital Mammography (IWDM 2002). Bremen, Germany, June 2002, pp 452–454

13. Oppenheim AV, Schafer RW: Discrete-Time Signal Processing. Englewood Cliffs, NJ: Prentice-Hall, 1996

14. Rabiner LR, McClellan JH, Parks TW: FIR digital filter design techniques using weighted Chebyshev approximation. Proc IEEE 63(4):595–610, 1975

15. Sunder S, Lu W-S, Antoniou A: Design of digital differentiators satisfying prescribed specifications using optimisation techniques. Proc IEEE 138(3):315–320, June 1991

16. Leung CM, Lu W-S: Detection of edges of noisy images by 1-D and 2-D linear FIR digital filters. In: IEEE Pacific Rim Conference on Communications, Computers and Signal Processing, vol. 1. pp 228–231, 1993

17. Kumar B, Dutta Roy SC: Design of digital differentiators for low frequencies. Proc IEEE 76(3):287–289, March 1988

18. Wong H, Antoniou A: One-dimensional signal processing techniques for airborne laser bathymetry. IEEE Trans Geosci Remote Sens 32(1):35–46, Jan. 1994

19. Selesnick IW: "Maximally flat low-pass digital differentiators." In: IEEE Trans. on Circuits and Systems—II: Analog and Digital Signal Processing, vol. 49, no. 3, March 2002

20. Compton K: Image Performance in CRT Displays. SPIE Press, Tutorial Text TT54, April 2003